Entanglement entropy and topological order in resonating valence-bond quantum spin liquids

Julia Wildeboer, Alexander Seidel, and Roger G. Melko

Phys. Rev. B **95**, 100402 — Published 6 March 2017

DOI: 10.1103/PhysRevB.95.100402

Entanglement Entropy and Topological Order in Resonating Valence-Bond Quantum Spin Liquids

Julia Wildeboer,[1,2] Alexander Seidel,[3,4] and Roger G. Melko[2,5]

[1] *Department of Physics and National High Magnetic Field Laboratory, Florida State University, Tallahassee, Florida 32310, USA*
[2] *Perimeter Institute for Theoretical Physics, Waterloo, Ontario, N2L 2Y5, Canada*
[3] *Department of Physics and Center for Materials Innovation, Washington University, St. Louis, Missouri 63130, USA*
[4] *Max-Planck-Institut für Physik komplexer Systeme, Nöthnitzer Str. 38, 01187 Dresden, Germany*
[5] *Department of Physics and Astronomy, University of Waterloo, Ontario, N2L 3G1, Canada*

On the triangular and kagome lattices, short-ranged resonating valence bond (RVB) wave functions can be sampled without the sign problem using a recently-developed Pfaffian Monte Carlo scheme. In this paper, we study the Renyi entanglement entropy in these wave functions using a replica-trick method. Using various spatial bipartitions, including the Levin-Wen construction, our finite-size scaled Renyi entropy gives a topological contribution consistent with $\gamma = \ln(2)$, as expected for a gapped $\mathbb{Z}_2$ quantum spin liquid. We prove that the mutual statistics are consistent with the toric code anyon model and rule out any other quasiparticle statistics such as the double semion model.

Introduction. – Two-dimensional frustrated quantum antiferromagnets can harbor a phase of matter called a quantum spin liquid; a state with no conventional symmetry but emergent, topological order [1, 2]. These phases are unique in that they exhibit gapped fractionalized quasiparticle excitations with exotic quantum statistics and ground state degeneracies on topologically nontrivial surfaces [3]. Although there is strong incentive to identify minimal theoretical models which possess topologically ordered phases, the fact that strong correlations are a crucial ingredient means that numerical methods necessarily play a large role. Numerical studies suffer several serious challenges. First, the vast majority of Hamiltonians and wave functions that may harbor candidate quantum spin liquid states are also afflicted with the "sign problem", precluding study by large-scale quantum Monte Carlo (QMC) [4]. Also, the absence of a local order parameter in a quantum spin liquid means that topological order must be characterized through more refined techniques, such as universal scaling terms in the entanglement entropy - the *topological* entanglement entropy (TEE) $-\gamma$ [5, 6]. Since γ is sub-leading to the diverging "area-law", it can be challenging to extract in numerical simulations [7–10]. Finally, distinct topological phases defined by different emergent quasiparticles can have the same TEE. To distinguish, one must rely on the modular $\mathcal{U}$ and $\mathcal{S}$-matrices, which encode information on the quasiparticle statistics of the underlying topological phase [11, 12].

In this Letter, we analyze the Renyi entanglement entropy of the short-ranged spin-$\frac{1}{2}$ resonating valence bond (RVB) wave function on the kagome and the triangular lattice. Recently Ref. [13] introduced a sign-problem free Pfaffian Monte Carlo scheme that can be used to produce unbiased samples of the singlet wave function, making it possible to evaluate local operators and their correlation functions. That work demonstrated that the RVB wave function on these two frustrated lattices has no local order parameter, and is gapped, consistent with expectations for an $SU(2)$-invariant quantum spin liquid. Here, we use the Pfaffian Monte Carlo technique to calculate the TEE, which explicitly shows $\gamma = \ln(2)$, as expected for a $\mathbb{Z}_2$ topologically-ordered phase. Further, we prove that the mutual statistics are consistent with the toric code anyon model in both the triangular and kagome RVB states, ruling out any other underlying anyon models such as the double semion.

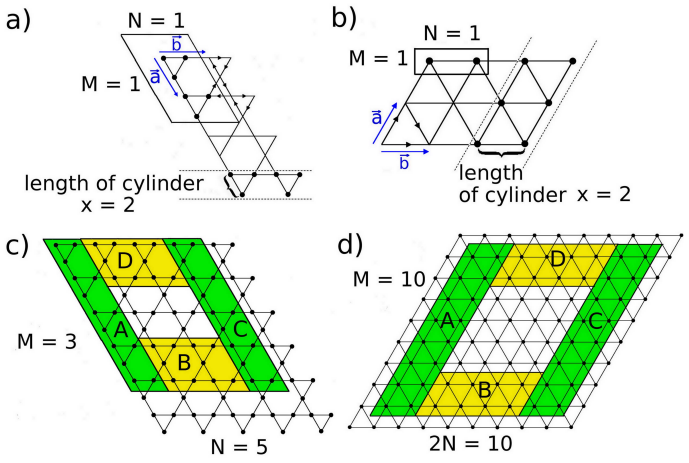

FIG. 1: a) The 6-site unit cell of the kagome lattice and the phase convention for singlets living on the lattice links. The length of the cylindrical regions that the entanglement entropy S_2 is measured over is shown as x. b) The 2-site unit cell, the respective phase convention and the definition of x for the triangular lattice. c) and d) show the Levin-Wen areas A, B, C and D for the kagome lattice of size $(M, N) = (3, 5)$ amounting to 90 sites, and the 10×10-triangular lattice, respectively. The TEE $-\gamma$ is obtained by a superposition of the EE of four areas: $-2\gamma = S_{ABCD} - S_{ABC} - S_{ADC} + S_{AC}$.

RVB Wave Functions, Entanglement, and QMC. – The RVB wave functions were conceived by Anderson 40

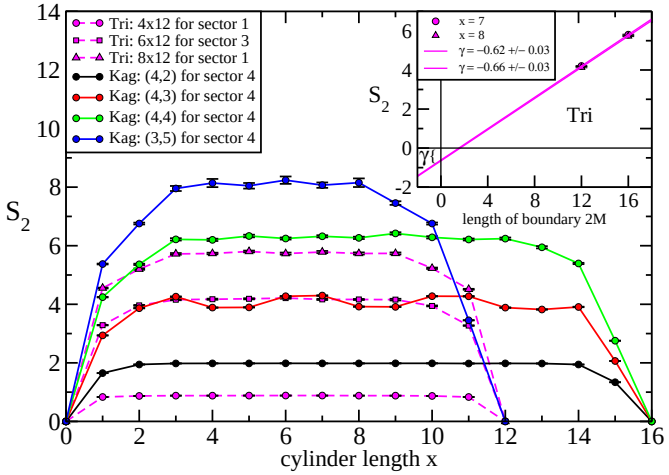

FIG. 2: The Renyi entropy S_2 for triangular (Tri) lattices of size $M \times 2N = 4, 6, 8 \times 12$ and kagome (Kag) lattices for various sizes (M, N) with total number of lattice sites $6MN$. There are four possible topological sectors for each wave function on a torus, each of which can be isolated independently in the Pfaffian MC. For the triangular lattice, the inset shows linear fits using S_2 from $M \times 2N = 6, 8 \times 12$ for lengths $x = 7, 8$ in order to extract γ' for a single sector. In total, we average over values stemming from fits for $4 \leq x \leq 8$, and obtain an average value of $-\gamma' = -0.64 \pm 0.07$.

years ago [14] for their variational appeal in demonstrating spin liquid physics. The simplest, nearest-neighbor RVB state represents a stable phase only on non-bipartite lattices. Although not typically discussed as ground states of explicit local Hamiltonians, RVB wave functions do sometimes allow for the construction of a local parent Hamiltonian, as notable in particular on the kagome lattice [15]. The uniqueness of the RVB-ground states, modulo a topological degeneracy, (demonstrated in Refs. [16, 17]) establishes that the Hamiltonian in Ref. [15] truly stabilizes the RVB state. In this work, we will directly consider the RVB wave function, defined via

$$|RVB\rangle = \sum_D |D\rangle \,. \tag{1}$$

Here, D goes over all possible pairings of a given lattice into nearest neighbor pairs ("dimer coverings"). Each site of the lattice is equipped with a spin-$\frac{1}{2}$ degree of freedom. For each dimer covering D, $|D\rangle$ denotes a state where each pair of lattice sites of the covering forms a singlet, where a sign convention is used that corresponds to an orientation of nearest neighbor links (see Fig. 1a & b). We note that the wave function Eq. (1) has a fourfold topological degeneracy on the torus for the kagome and triangular lattices.

Like in any quantum wave function, the properties of an RVB state can be investigated through its bipartite entanglement entropy, where the lattice is divided into a region A and its complement B. The Renyi entropy of order n is defined as $S_n = \ln \mathrm{Tr}(\rho_A^n)/(1-n)$, where $\rho_A = \mathrm{Tr}_B |\Psi\rangle\langle\Psi|$ is the reduced density matrix of region A. Ground states of local Hamiltonians are known to exhibit a *area law* scaling in region size, which in two dimensions can generically be written as, $S_n(\rho_A) = \alpha_n L_A - \gamma + \cdots$ [18]. Here, the leading term is dependent on the "area" (or boundary) of region A. The second term, the topological entanglement entropy (TEE) $-\gamma$ [5, 6], is characterized by the total quantum dimension $\mathcal{D}$, which is defined through the quantum dimensions of the individual quasiparticles d_i of the underlying theory: $\mathcal{D} = \sqrt{\sum_i d_i^2}$ [5, 6, 19]. Conventionally ordered phases have $\mathcal{D} = 1$, while topologically ordered phases have $\mathcal{D} > 1$ with the TEE given by $-\gamma = -\ln(\mathcal{D})$.

Note that in the case where the area A has at least one non-contractible boundary, such as a cylinder (see Fig. 1a & b), γ becomes state-dependent. As shown in Ref. [11], if one expresses any state in the basis of the *minimum entropy states* (MES-states), $|\Psi_\alpha\rangle = \sum_j c_j |\Xi_j\rangle$, then the sub-leading constant to the area law from a two-cylinder cut is,

$$\gamma'(\{p_j\}) = 2\gamma + \ln\left(\sum_j \frac{p_j^2}{d_j^2}\right) . \tag{2}$$

for S_2, where $p_j = |c_j|^2$. We further discuss MES-states in the results to follow.

In contrast to bipartite lattices [20–27], RVB states on non-bipartite lattices are not amenable to valence-bond QMC; they have been studied previously by PEPs representations [28–30], but should also be accessible to QMC if a sign-problem free sampling method can be constructed [13, 31, 32]. Here, we investigate entanglement properties of the spin-$\frac{1}{2}$ RVB wave functions using the variational Pfaffian MC scheme for lattices of up to 128 sites. Note that the Pfaffian MC scheme allows one to project onto each topological sector, and every linear combination thereof. We will use this feature in the following results. To obtain the second Renyi entropy S_2 for contractible and noncontractible regions, we employ the standard QMC replica-trick [33, 34]. We refer to Refs. [13, 35] for more details on the method.

Measurements of TEE. – We begin by calculating the TEE using boundaries for region A that are contractible around the toroidal lattice. To isolate γ, we perform a Levin-Wen bipartition [5], which was successfully used previously to detect a $\mathbb{Z}_2$ quantum spin liquid using QMC simulations on toroidal lattices of restricted finite-size [7]. We obtain data for such bipartitions on both a triangular RVB of size $M \times 2N = 10 \times 10$ and two kagome RVBs with $(M, N) = (3, 5), (3, 6)$ amounting to 90 and 108 sites, respectively. The triangular lattice and the $(3, 5)$-kagome geometries are shown in Fig. 1, which also shows the Levin-Wen regions A, B, C, D used to obtain γ [5]. For the $(3, 6)$-kagome, the $A(C)$ regions are the same as in $(3, 5)$, whereas the regions $B(D)$ are one link longer in N-direction than in $(3, 5)$. Using this procedure, the triangular lattice gives $-\gamma \approx -0.80 \pm 0.2$, while for the kagome, we end up with $-\gamma = -0.89 \pm 0.22, -0.74 \pm 0.34$ for $(3, 5)$ and $(3, 6)$, respectively.

To improve accuracy, we now consider regions with non-contractible boundaries. We examine a triangular lattice RVB for fixed $2N = 12$ and $M = 4, 6, 8$, and a kagome lattice RVB of size $6MN$ with $M = 4$ and $N = 2, 3, 4$. We subsequently calculate the Renyi entropy S_2 for cylindrical bipartitions (see Fig. 1). As the cylinder length increases, S_2 quickly saturates (Fig. 2). This type of behavior is consistent with the system having a gap. We point out that, as expected, several curves in Fig. 2 exhibit finite size effects, manifest clearly in the different S_2 for different topological sectors. This can be seen in Fig. 3, 7 and 8 [35].

Figure 3 and Figures 7, 8 in the SM demonstrate that, for large enough system sizes, S_2 does not depend on the topological sector for these two wave functions. The four topological sectors $|\Psi_i\rangle$ of each wave function can be distinguished by their two quantum numbers, $i = \{ee, eo, oe, oo\}$, which are the even (e) or odd (o) number of dimers cut along the two directions $\vec{a}$ and $\vec{b}$. One can make use of special linear combinations of these topological sectors to devise another method of determining the TEE $-\gamma$. Here, we choose as a compatible ansatz for $\mathbb{Z}_2$ spin liquids the minimal-entangled states (MES) obtained for the toric code and the dimer model on kagome/triangular lattices [11, 35] and examine its properties. These MES-states for cuts along $\vec{b}$ are, up to a phase $e^{i\Phi_j}$,

$$|\Xi_{1,2}\rangle = \frac{1}{\sqrt{2}}(|\Psi_{ee}\rangle \pm |\Psi_{eo}\rangle) \ ,$$
$$|\Xi_{3,4}\rangle = \frac{1}{\sqrt{2}}(|\Psi_{oe}\rangle \pm |\Psi_{oo}\rangle) \ . \qquad (3)$$

We apply this ansatz to our Pfaffian QMC data. First, consider slices (of constant cylinder length x) through the triangular lattice to obtain a plot of $S_2(L_{2M}) = \alpha L_{2M} - \gamma'$, as in the inset of Fig. 2. The intercept of this plot is $-\gamma'$ which is now the state dependent TEE; we numerically extract $-\gamma' = -0.64 \pm 0.07$. We can thus obtain the TEE using Eq. (2). First note that, as seen in Fig. 4 of the SM, the entropy S_2 does not depend on which MES-state is used (within error bars), which implies that d_j is also the same for all four MES-states. Since every theory, Abelian and non-Abelian, contains (at least) one quasiparticle with quantum dimension unity, we conclude that all quasiparticle dimensions are necessarily $d_j = 1$. Since the p_j are fixed to be $1/4$ by our ansatz Eq. (3), then for the single sector plotted in Fig. 2, $\gamma' = 2\gamma + \ln(1/4 + 1/4)$. Thus, we conclude that $\gamma = 0.67 \pm 0.04$ consistent with $\mathbb{Z}_2$ topological order.

Next we turn to the kagome lattice RVB. As seen in Fig. 3 (inset) and Fig. 8 in the SM [35], it takes a system of size $(M, N) = (4, 3)$ to eliminate finite-size effects and reach agreement of S_2 of all four topological sectors within error bars. Since larger system sizes can become computationally expensive, an extraction of γ' using the procedure of Fig. 2 becomes more difficult. Alternatively, as discussed in Ref. [11], linear superpositions of different

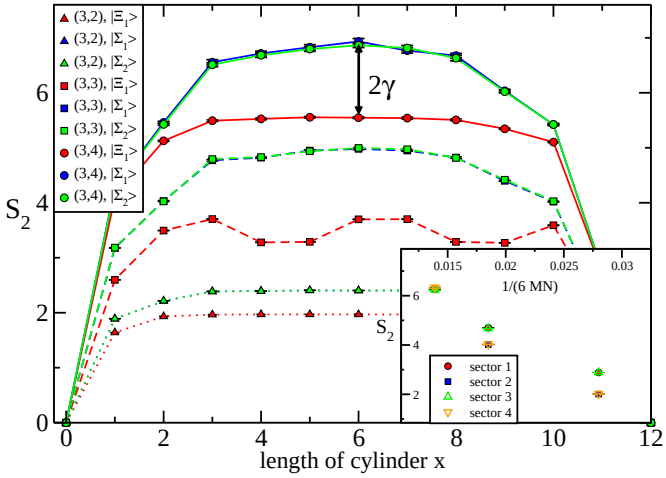

FIG. 3: S_2 for kagome-lattice MES-state ($|\Xi_1\rangle$) which is a specific superposition of two topological sectors for different lattice sizes and for two respective nonMES-states ($|\Sigma_{1,2}\rangle$). The difference between $(M, N) = (3, 4)$ for the two nonMES-states compared to the MES-state has to be $2\gamma = 2\ln(2) \approx 1.38$. If we average over differences obtained for lengths $x = 5, 6, 7$, we get $-\gamma' = -2\gamma = -1.36 \pm 0.13$. The inset shows a comparison of S_2 for cylindrical regions between sectors $1, 2, 3, 4$ on the kagome lattice. We observe that for large enough system sizes $(M, N) = (3, 4)$ amounting to 72 lattice sites, the EE S_2 is the same for all four sectors within errors.

MES states can be used to extract all information about the topological order from our measurement. Specifically, the linear combination of all four MES-states,

$$|\Sigma_{1,2}\rangle = \frac{1}{\sqrt{2}}(|\Psi_{ee}\rangle + |\Psi_{oe(oo)}\rangle)$$
$$= \frac{1}{2}\Big(|\Xi_1\rangle + |\Xi_2\rangle + |\Xi_3\rangle \pm |\Xi_4\rangle\Big), \qquad (4)$$

will have $\gamma' = 0$ according to Eq. (2). Here, index 1 (2) corresponds to oe (oo), and $+$ ($-$) in the second line.

We investigate the behavior of S_2 for the MES-state, Eq. (3), and the nonMES-states, Eq. (4), for the kagome lattice RVB. We first note that the numerical data of Fig. 3 (Figs. 7, 8 in the SM) suggests S_2 to be independent of MES-state (once finite-size effects are accounted for). Since S_2 is similarly the same across all four topological sectors, this implies that γ' is the same for all $|\Xi_i\rangle$ and for all $|\Psi_i\rangle$, respectively. The latter means that each of the four quasi-particles belonging to the four MES-states have the same quantum dimension. Since every phase, Abelian and non-Abelian, has (at least) one quasiparticle with quantum dimension $d = 1$, this implies that all quasi-particles have $d_i = 1$, indicating the Abelian nature of the phase. We calculate the difference in S_2 between MES (3) and nonMES (4) states by performing an average over cylinder lengths $x = 4, \ldots, 8$, and obtain $-\gamma' = -1.36 \pm 0.13$. This matches the expectation from Eq. (2) that this difference should be $-2\gamma \approx -1.38$, confirming that the MES ansatz is also correct for the

kagome-lattice RVB.

Quasiparticle Statistics. – We point out that the numerical confirmation of the MES-states ansatz Eq. (3) essentially determines the topological order of our system, and in particular distinguishes between toric code and double semion topological order as we now explain. We consider the matrices $\mathcal{S}$ and $\mathcal{U}$, which describe the quasiparticle statistics of the system and correspond to modular transformations of the same name at the level of the effective field theory. In a microscopic lattice model, the corresponding transformations cannot necessarily be realized as discrete symmetry operations. However, for both the kagome and the triangular lattice, the transformation corresponding to $\mathcal{US}^{-1}$ is realized as the symmetry under a $\pi/3$-rotation [35], as long as the lattice dimensions are chosen to be of the form $(M, N) = (M, 2M)$ or $(M, 2N) = (2N, 2N)$ for the kagome or triangular, respectively. Up to a phase ambiguity [11], the matrix elements $V_{ij} = \langle \Xi_i | R_{\pi/3} | \Xi_j \rangle$ are thus equal to those of the matrix $\mathcal{US}^{-1}$, where $R_{\pi/3}$ represents the $\pi/3$-rotation. We therefore must have $V_{ij} = D^\dagger \mathcal{US}^{-1} D$, where D is a diagonal matrix of phases $D_{jj} = e^{i\Phi_j}$ corresponding to the phase ambiguity. V_{ij} is easily calculated from Eq. (3) by working out the transformation properties of the states $|\Psi_{\alpha,\beta}\rangle$ under rotation [35, 36]. It is manifestly real, as is $\mathcal{US}^{-1}$ for the toric code, and we find agreement for $D_{jj} = 1$ for all jj's. In contrast, for the double semion model, $\mathcal{US}^{-1}$, while having the same eigenvalues as in the toric code case, we note that $\mathcal{U}$ has some purely imaginary diagonal entries. Therefore, in the double semion case, $D^\dagger \mathcal{US}^{-1} D$ must have imaginary entries for any choice of D, and agreement with our MES-states cannot be achieved.

Thus, the MES-states we identified demonstrate the underlying quasiparticle statistics to be consistent with the toric code model, ruling out any other statistics, in particular double semion statistics.

Conclusion. – In this work, we have used a sign-problem free Pfaffian quantum Monte Carlo (QMC) to calculate the second Renyi entropy of the nearest-neighbor RVB wave function on the triangular and kagome lattices. Through a bipartition of each lattice into Levin-Wen [5] regions, and cylindrical regions, we confirm that the topological entanglement entropy (TEE) is consistent with $-\gamma = -\ln(2)$, the value for a $\mathbb{Z}_2$ quantum spin liquid. Finite-size scaling of the two-cylinder Renyi entropy for the triangular lattice and comparisons between S_2 for different wave functions in MES-basis for the kagome, confirm the ansatz MES-states taken for a $\mathbb{Z}_2$ topological gauge structure. Further, we identify the nature of the anyonic quasiparticles to be of toric code type, by explicitly showing that our numerically confirmed MES-states ansatz leads to the modular $\mathcal{US}^{-1}$-matrix of the toric code statistics and rules out any other quasiparticle statistics including double semion statistics.

This work serves as an important example that all aspects of quantum spin liquid behavior, from the initial demonstration of the liquid nature [13] to the characterization of the emergent gauge structure through the TEE, to the full determination of the underlying statistics and braiding of fractional quasiparticle excitations, can be performed with un-biased QMC techniques. Thus, the $SU(2)$-invariant RVB states on triangular and kagome lattices add to the growing list of wave functions and Hamiltonians that have been demonstrated to exist, and can be simulated in practice, on non-bipartite lattices without being vexed by the sign-problem [4, 37].

Finally, we emphasize that our results rely crucially on the numerical extraction of the second Renyi entropy of the quantum ground state. For RVB wave functions (and all other many-body systems), the replica-trick method used here [33] is the same as that employed in recent experiments on interacting ^{87}Rb atoms in a one-dimensional optical lattice [38]. Hence, the concepts and techniques used in this paper will be important for efforts to characterize topological order in synthetic quantum matter in the near future.

Acknowledgments

The authors are indebted to J. Carrasquilla, Ch. Herdman, and E. M. Stoudenmire for enlightening discussions. We are especially indebted to L. Cincio for several critical readings of the manuscript. AS would like to thank K. Shtengel for insightful discussions. Our MC codes are partially based upon the ALPS libraries [39, 40]. This work has been supported by the National Science Foundation under NSF Grant No. DMR-1206781 (AS), NSERC, the Canada Research Chair program, and the Perimeter Institute (PI) for Theoretical Physics. Research at Perimeter Institute is supported by the Government of Canada through Industry Canada and by the Province of Ontario through the Ministry of Research and Innovation. JW is supported by the National High Magnetic Field Laboratory under NSF Cooperative Agreement No. DMR-0654118 and the State of Florida.

[1] X. G. Wen, Int. J. Mod. Phys. **B4**, 239 (1990).
[2] X.-G. Wen, ISRN Condensed Matter Physics **2013**, 198710 (2013).
[3] L. Balents, Nature **464**, 199 (2010).
[4] R. K. Kaul, R. G. Melko, and A. W. Sandvik, Annual Review of Condensed Matter Physics **4**, 179 (2013).
[5] M. Levin and X.-G. Wen, Physical Review Letters **96**, 110405 (2006).
[6] A. Kitaev and J. Preskill, Phys. Rev. Lett. **96**, 110404 (2006).

[7] S. V. Isakov, M. B. Hastings, and R. G. Melko, Nature Physics **7**, 772 (2011).
[8] Y. Zhang, T. Grover, and A. Vishwanath, Physical Review B **84**, 075128 (2011).
[9] T. Grover, Y. Zhang, and A. Vishwanath, New Journal of Physics **15**, 025002 (2013).
[10] W. Zhu, S. Gong, and D. Sheng, Journal of Statistical Mechanics: Theory and Experiment **2014**, P08012 (2014).
[11] Y. Zhang, T. Grover, A. Turner, M. Oshikawa, and A. Vishwanath, Physical Review B **85**, 235151 (2012).
[12] L. Cincio and G. Vidal, Physical Review Letters **110**, 067208 (2013).
[13] J. Wildeboer and A. Seidel, Physical Review Letters **109**, 147208 (2012).
[14] P. W. Anderson, Mater. Res. Bull **8**, 153 (1973).
[15] A. Seidel, Physical Review B **80**, 165131 (2009).
[16] N. Schuch, I. Cirac, and D. Pérez-García, Annals of Physics **325**, 2153 (2010).
[17] Z. Zhou, J. Wildeboer, and A. Seidel, Physical Review B **89**, 035123 (2014).
[18] J. Eisert, M. Cramer, and M. B. Plenio, Rev. Mod. Phys. **82**, 277 (2010).
[19] S. Dong, E. Fradkin, R. G. Leigh, and S. Nowling, Journal of High Energy Physics **2008**, 016 (2008).
[20] B. Sutherland, Physical Review B **37**, 3786 (1988).
[21] S. Liang, B. Doucot, and P. W. Anderson, Physical Review Letters **61**, 365 (1988).
[22] A. W. Sandvik, Phys. Rev. Lett. **95**, 207203 (2005).
[23] A. F. Albuquerque and F. Alet, Physical Review B **82**, 180408 (2010).
[24] Y. Tang, A. W. Sandvik, and C. L. Henley, Physical Review B **84**, 174427 (2011).
[25] H. Ju, A. B. Kallin, P. Fendley, M. B. Hastings, and R. G. Melko, Physical Review B **85**, 165121 (2012).
[26] J.-M. Stéphan, H. Ju, P. Fendley, and R. G. Melko, New Journal of Physics **15**, 015004 (2013).
[27] M. Punk, A. Allais, and S. Sachdev, arXiv preprint arXiv:1501.00978 (2015).
[28] F. Verstraete, M. M. Wolf, D. Perez-Garcia, and J. I. Cirac, Phys. Rev. Lett. **96**, 220601 (2006).
[29] N. Schuch, D. Poilblanc, J. I. Cirac, and D. Pérez-García, Phys. Rev. B **86**, 115108 (2012).
[30] M. Iqbal, D. Poilblanc, and N. Schuch, Phys. Rev. B **90**, 115129 (2014).
[31] F. Becca, L. Capriotti, A. Parola, and S. Sorella, in *Introduction to Frustrated Magnetism* (Springer, 2011), pp. 379–406.
[32] F. Yang and H. Yao, Phys. Rev. Lett. **109**, 147209 (2012).
[33] M. B. Hastings, I. González, A. B. Kallin, and R. G. Melko, Physical Review Letters **104**, 157201 (2010).
[34] A. B. Kallin, M. B. Hastings, R. G. Melko, and R. R. P. Singh, Phys. Rev. B **84**, 165134 (2011).
[35] See the Supplemental Material.
[36] D. Poilblanc and G. Misguich, Physical Review B **84**, 214401 (2011).
[37] R. K. Kaul, Phys. Rev. Lett. **115**, 157202 (2015).
[38] R. Islam, R. Ma, P. M. Preiss, M. E. Tai, A. Lukin, M. Rispoli, and M. Greiner, Nature **528**, 77 (2015).
[39] M. Troyer, B. Ammon, and E. Heeb, *Parallel Object Oriented Monte Carlo Simulations* (Springer, 1998).
[40] A. Albuquerque, F. Alet, P. Corboz, P. Dayal, A. Feiguin, S. Fuchs, L. Gamper, E. Gull, S. Gürtler, A. Honecker, et al., Journal of Magnetism and Magnetic Materials **310**, 1187 (2007).